energy&fuels

ARTICLE

pubs.acs.org/EF

Carbon Dioxide Capture Using Calcium Hydroxide Aqueous Solution as the Absorbent

Sang-Jun Han, Miran Yoo, Dong-Woo Kim, and Jung-Ho Wee*

Department of Environmental Engineering, The Catholic University of Korea, 43-1, Yeokgok 2-dong, Wonmi-gu, Bucheon-si, Gyeonggi-do 420-743, Republic of Korea

ABSTRACT: Although $Ca(OH)_2$ aqueous solution can be effectively used as an absorbent to capture CO_2, its performance with highly concentrated CO_2 gas mixtures has rarely been reported. Therefore, the present paper investigates the CO_2-capture performance of $Ca(OH)_2$ aqueous solution for an about 30% CO_2 gas mixture. The $Ca(OH)_2$ concentration in the solution strongly influenced the capture performance of the absorbent. The simultaneous $Ca(OH)_2$ dissolution and $CaCO_3$ production in the absorbent may have substantially hindered the combination of Ca^{2+} with CO_3^{2-} in suspension. Therefore, a higher $Ca(OH)_2$ concentration in suspension further reduced the CO_2 absorption capacity and produced substantially agglomerated $CaCO_3$ with low crystallinity. In contrast, the $Ca(OH)_2$-saturated aqueous solution had the highest absorption rate and capture ratio among the six investigated absorbents. Its calculated absorption capacity of 3.05 g of CO_2 [g of $Ca(OH)_2]^{-1}$ L^{-1} was 3-fold more than that of 1% $Ca(OH)_2$ suspension solution, which confirmed $Ca(OH)_2$-saturated aqueous solution as the most efficient absorbent for CO_2 in a $Ca(OH)_2$ aqueous solution system.

1. INTRODUCTION

Extensive efforts have recently been expended worldwide to address global climate change. Carbon dioxide (CO_2) capture and storage (CCS) may be a viable and promising technology to effectively reduce CO_2 emissions into the atmosphere. According to Intergovernmental Panel on Climate Change (IPCC) reports,[1] CCS will be able to decrease CO_2 emissions by between 15 and 55% by 2100. The outstanding achievements that have been reported in the specific field of CO_2 capture are increasing the potential for CCS technology to significantly contribute to CO_2 emission reduction. At a minimum, CCS will provide a temporary solution until renewable and sustainable energy streams become fully developed and widely used.

Among the many options for CO_2-capture technology, absorption is almost the only presently commercialized process. Chemical absorption using amine-based absorbents, such as monoethanolamine (MEA) and diethanolamine (DEA),[2,3] is currently adopted in most post-combustion plants. MEA was developed over 70 years ago as a general absorbent[4] to remove various acid gases, including CO_2 and H_2S, from natural gas streams. However, with the emergence of the CO_2 issue in the 1990s,[5,6] advanced absorption using MEA has begun to receive greater attention for CO_2 capture. Therefore, many papers[2,7−12] have focused on its performance, economies, and availability. Despite its commercialization, many process problems remain, including solvent degradation, equipment corrosion, and high energy consumption for solvent recovery.

CO_2 fixation via the production of insoluble carbonate salts, such as via the carbonation of a caustic solution absorbing CO_2, is another option for CO_2 capture. $Ca(OH)_2$ aqueous solution is used as an effective solvent to absorb CO_2 because of its various advantageous features. First, Ca is inexpensive, abundant, and non-hazardous. $CaCO_3$ precipitation from the carbonation of $Ca(OH)_2$ aqueous solution is a very familiar and classic reaction commonly observed in nature.[13−16] Second, reclamation and regeneration are available to dispose the produced $CaCO_3$. Closed reclamation in a restricted area has become an environmentally friendly and long-term storage option. The direct reclamation of $CaCO_3$ may be more economic than traditional CO_2 sequestration because of the absence of any additional cost for CO_2 liquefaction and transportation.

However, $Ca(OH)_2$ aqueous solution has not received much attention for CO_2 capture because of two limitations. First, the source of $Ca(OH)_2$ (or CaO) has mostly been natural limestone, but the extraction process is very energy-intensive, which itself leads to greatly increased CO_2 emissions. The second issue is the disposal of the large amounts of $CaCO_3$ and water mixture that are produced. Therefore, most studies on $Ca(OH)_2$ carbonation have solely examined the synthesis of precipitated $CaCO_3$.[17−20]

However, many advanced technologies have recently been developed to address these problems. Many papers have focused on the search for alternative Ca sources, including Ca extraction from wollastonite ($CaSiO_3$)[21−23] and from the calcium silicate (Ca_2SiO_4) existing in various industrial residues, such as municipal solid waste incinerator,[24,25] ash, and steel slag.[26,27] In addition, many studies have recently reported on the CaO generation from $CaCO_3$ by thermal dissociation, which is called Ca looping.[28−36] Although, many challenges remain because of the energy intensity of the process and the temperature required for calcination, it has a strong potential because high-temperature waste heat (for example, from solid oxide fuel cells[37] or molten carbonate fuel cells[38]) or concentrated solar energy[35] can be effectively used for $Ca(OH)_2$ generation.

With regard to the disposal of produced $CaCO_3$ and water, the constant supply of $Ca(OH)_2$ or CaO powders to the absorber can substantially reduce the mixture volume and, finally,

Received: March 17, 2011
Revised: June 19, 2011
Published: June 20, 2011

decantation may be effectively used to separate them. Water can be recycled for CaO hydration in Ca looping, and heat absorbed into water during carbonation can be recovered in any process. In addition, the $Ca(OH)_2$ aqueous solution can be used in spray dryers to capture CO_2 without water.[15] Therefore, considering these effects and the current importance of CO_2 emission reduction, the $Ca(OH)_2$ carbonation reaction deserves research attention as a CCS technology. Therefore, many papers have already reported the performance of the $Ca(OH)_2$ aqueous solution as an absorbent to directly capture CO_2. In particular, many works have examined CO_2 absorption from the atmosphere, termed air capture.[31,39−41] However, the process has rarely been applied to localize points with medium or highly concentrated CO_2 emissions, such as the cement plant and anode outlet combustion gas of molten carbonate fuel cell.

Therefore, the present paper reports the CO_2-capture performance of $Ca(OH)_2$ aqueous solution in a gas mixture with a relatively high CO_2 concentration of about 30% (balance N_2) at ambient temperature. Several absorbents, including $Ca(OH)_2$-saturated aqueous and suspension solutions comprising different amounts of $Ca(OH)_2$, are prepared, and the absorption is carried out in a batch reactor. On the basis of the measured variation of the CO_2 composition in the outlet gas, electrical conductivity (EC), and pH during absorption, the absorption capacity, absorption time, rate, and capture efficiency of the absorbents are calculated. In addition, the optimum condition for CO_2 capture is reported, and the absorption mechanism in the absorbents is analyzed over a wide pH range.

2. THEORY

The overall reaction for CO_2 capture using $Ca(OH)_2$ aqueous solution is expressed as eq 1

$$Ca(OH)_2(s) + CO_2(g) \leftrightarrow CaCO_3(s) + H_2O(l), \quad \Delta H^{\circ}_{298\ K} = -109\ kJ/mol \tag{1}$$

The reaction is thermodynamically favorable in the temperature range from ambient to 750 °C, and the reaction rate is very fast in aqueous solution.[13,42] Produced $CaCO_3$ can be reclaimed to a limited extent or regenerated to $Ca(OH)_2$ by calcination and hydration (or slaking).

2.1. Individual Reactions during CO_2 Absorption. Reaction 1 includes many individual reactions, such as $Ca(OH)_2$ dissolution and HCO_3^- production. Some individual reactions proceed irrespective of the pH, while others are restricted to a specific pH range. They are summarized as follows.

(1) $Ca(OH)_2$ dissolution reaction: The $Ca(OH)_2$ dissolution reaction in water is expressed as eq 2.

$$Ca(OH)_2(s) \leftrightarrow Ca^{2+}(aq) + 2OH^-(aq) \tag{2}$$

The solubility of $Ca(OH)_2$ in water is negatively correlated with the temperature, as denoted in the following equation:[43,44]

$$\text{solubility of } Ca(OH)_2\ (g/kg \text{ of solution}) = -0.0108T\ (°C) + 1.7465$$

Therefore, the solubility at 25 °C is 1.48 g/kg of solution. This reaction can be the rate-controlling step of the overall reaction.[45] Dissociated OH^- is reacted with aqueous CO_2 in water to produce carbonic acid ion. The carbonic acid ion primarily exists in the form of CO_3^{2-} and HCO_3^- in the pH ranges of pH > 10.5 and 6.5 < pH < 10.5, respectively. At pH < 6.5, $H_2CO_3(aq)$ is the main constituent. Therefore, $CaCO_3$ is not precipitated at pH under 10 because of the absence of CO_3^{2-}. Meanwhile, produced $CaCO_3$ is slightly dissolved in acidic condition at pH under 6.5.[46]

(2) Individual reactions proceed across the pH range: These are listed as eqs 3−6.

$$CO_2(g) \leftrightarrow CO_2(aq) \tag{3}$$

$$CO_2(aq) + H_2O(l) \leftrightarrow H_2CO_3(aq) \tag{4}$$

$$H_2CO_3(aq) \leftrightarrow H^+(aq) + HCO_3^-(aq) \tag{5}$$

$$HCO_3^-(aq) \leftrightarrow H^+(aq) + CO_3^{2-}(aq) \tag{6}$$

Reactions 3 and 5 are very fast. Reaction 4 can be rate-controlling because its rate is relatively slow, except at high pH. Reaction 6 is faster than reaction 4 and slower than reaction 5.[47,48]

(3) Individual reactions proceed in 10 < pH < initial value (high): Reactions 7−9 are possible in this range.

$$CO_2(aq) + OH^-(aq) \leftrightarrow HCO_3^-(aq) \tag{7}$$

$$HCO_3^-(aq) + OH^-(aq) \leftrightarrow H_2O(l) + CO_3^{2-}(aq) \tag{8}$$

$$Ca^{2+}(aq) + CO_3^{2-}(aq) \leftrightarrow CaCO_3(s) \tag{9}$$

The rate of reaction 8 is even faster than that of reaction 7,[46] and reaction 9 is known to be instantaneous.[45] Therefore, reaction 7 can be the rate-controlling step in this range.[49] $CaCO_3$ is produced according to reaction 9, in which the nucleation of $CaCO_3$ at pH over 12.5[50] is followed consecutively by precipitation and growth until pH 10.[46]

(4) Individual reactions proceed in 7 < pH < 10: Two reactions 7 and 8 are also possible in this range. However, reaction 7 is faster than reaction 8, which leads to an even higher concentration of HCO_3^- than CO_3^{2-} in solution. Therefore, $CaCO_3$ is rarely produced in this range.[46]

(5) Individual reaction in pH < 7: As the HCO_3^- and H^+ concentrations are increased in the previous range, the solution becomes more acidic in accordance with reaction 10, leading to the dissolution of a slight amount of $CaCO_3$ according to reaction 11.[51]

$$H_2CO_3(aq) + CO_3^{2-}(aq) \leftrightarrow 2HCO_3^-(aq) \tag{10}$$

$$CaCO_3(s) + HCO_3^-(aq) + H^+(aq) \leftrightarrow Ca^{2+}(aq) + 2HCO_3^-(aq) \tag{11}$$

$CaCO_3$ begins to be dissolved in the form of $Ca(HCO_3)_2$, which is a more easily soluble substance. If CO_2 is continuously supplied to the solution, the $CaCO_3$ dissolution continues during the quasi-equilibrium state[46] and finally ceases at equilibrium.[50]

3. EXPERIMENT AND CALCULATION

Six kinds of absorbents were prepared for CO_2 capture. The first, named 1 g-F, comprised 0.5 L of $Ca(OH)_2$-saturated aqueous solution, in which $Ca(OH)_2$ (Samchun Chemical Co., 95%) was dissolved to its maximum solubility of 0.7383 g in 500 g of pure water at 25 °C.[42,43] This was prepared by filtering $Ca(OH)_2$ suspension solution. The other five, named 1 g-S−5 g-S, were 0.5 L of $Ca(OH)_2$ suspension solutions with 1, 2, 3, 4, and 5 g of $Ca(OH)_2$, respectively. In all suspension absorbents, 0.7383 g of $Ca(OH)_2$ was commonly dissolved and any excess coexisted

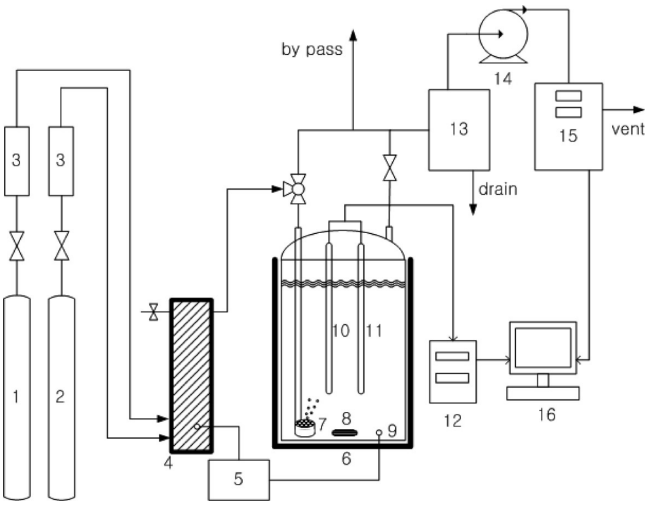

Figure 1. Schematic diagram for a CO_2-capture system using $Ca(OH)_2$ aqueous solution as the absorbent: (1) N_2 cylinder, (2) CO_2 cylinder, (3) MFC, (4) gas mixer, (5) temperature controller, (6) Pyrex reactor, (7) sparser, (8) magnetic stirrer, (9) thermometer, (10) pH sensor, (11) EC sensor, (12) pH/EC meter, (13) dehumidifier, (14) sampling pump, (15) gas analyzer, and (16) computer for data acquisition.

in the undissolved state. Figure 1 shows a schematic diagram of the absorption.

A cylindrical Pyrex reactor (D, 110 mm; h, 80 mm) was employed as an absorber and filled with 0.5 L of absorbents. A stirrer bar was constantly rotated at the speed of 180 rpm in the solution to ensure uniformly distributed absorption. The feed gas was a mixture of purified CO_2 and N_2. The two gases were sufficiently mixed in a gas mixer at a constant temperature. The two gas flow rates were controlled by a mass flow controller (MFC) at 1 L/min for CO_2 and 2 L/min for N_2. CO_2 composition of the gas mixture was 30.2% (by volume) using a non-dispersive infrared (NDIR)-based gas analyzer (maMos-200, Madur Electronics).

Before absorption was conducted, most parts of the experimental apparatus, including the gas line, empty space of the absorber, and even the absorbents themselves, were washed by N_2 purging. Thereafter, the gas mixture was sufficiently bypassed to stabilize the gas composition and flow rate. Absorption was conducted by injecting the gas mixture into the absorber at a flow rate of 3 L/min through a sparser, as shown in Figure 1.

Outlet gas from the absorbent was condensed to remove any water vapor, and the gas was supplied to the gas analyzer at a flow rate of 1.5 L/min by a built-in pump that vented any remaining outlet gas. The CO_2 composition in the outlet gas was measured every 1 s using a gas analyzer, and the data were directly acquired by a computer. The amount of CO_2 absorbed in the absorbent was calculated on the basis of the outlet CO_2 composition, gas flow rate, and unchanged absolute amount of fed N_2. Therefore, the amount of CO_2 absorbed until the time of t is calculated according to eq 12

$$Q_{C,t} = \sum_{t=0}^{final-1} \left(C_o - \frac{(C_t + C_{t+1})}{2} \right) \dot{V} \qquad (12)$$

where $Q_{C,t}$ is the amount of CO_2 absorbed until the time of t, t is the finite element time (constant; 1 s), C_o is the initial CO_2 concentration in the gas mixture, C_t is the outlet CO_2 concentration at time t, and $\dot{V}$ is the gas flow rate fed to gas mixer (constant; 0.05 L/s).

The EC and pH variation in the absorbent during the absorption were measured every 5 s using a pH/EC meter (Orion 4 Star, Thermo Scientific) and a computer.

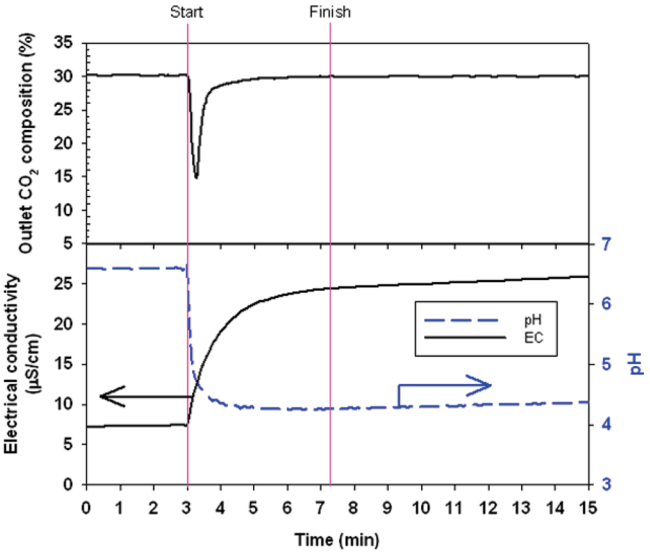

Figure 2. Variation of outlet CO_2 composition, EC, and pH in pure water according to CO_2 absorption time.

The absorption completion point was determined on the basis of solely the outlet CO_2 composition. Although EC was continuously varied, CO_2 absorption was considered completed once the outlet CO_2 composition from the absorbent reached the initial value. Every experimental result is the average value of three or seven runs. $CaCO_3$ produced by the absorption was analyzed using X-ray diffraction (XRD) (D5000, Siemens) and scanning electron microscopy (SEM) (S-4800, Hitachi).

4. RESULTS AND DISCUSSION

4.1. CO_2 Absorption in Pure Water. Figure 2 shows the results of the CO_2 absorption into pure water at 25 °C.

The initial pH and EC were 6.59 and 7.47 μS/cm, respectively. As the CO_2 was absorbed, reactions 3−6 proceeded, leading to a decrease in pH and an increase in EC until CO_2 saturation. In the experiment, the final pH and EC in the CO_2-saturated pure water were 4.27 and 24.40 μS/cm, respectively. Although EC was increased to 25.90 μS/cm at 13 min from the start, the absorption time, i.e., the point at which the outlet CO_2 composition equaled the initial value, was only 4 min and 16 s. Therefore, 0.52 g of CO_2/0.5 L of water was absorbed in the pure water, which was regarded as the standard solubility of CO_2 at the partial pressure of $^1/_3$ atm at 25 °C.

4.2. CO_2 Absorption in $Ca(OH)_2$-Saturated Aqueous Solution. Figure 3a shows the changes of outlet CO_2 composition, pH, and EC according to absorption time when CO_2 was absorbed in 1 g-F.

At this time, the dependence of the individual reactions upon the pH can be explained as follows.

(1) 10 < pH < initial: Reaction 2 did not proceed because 1 g-F was prepared by filtering the $Ca(OH)_2$ suspension solution. CO_2 absorption began at an initial pH of 12.99 and initial EC of 7160 μS/cm. In this pH range, reactions 3−9 proceeded as described in the Theory section. In particular, reaction 8 dominated, leading to $CaCO_3$ precipitation according to reaction 9. Furthermore, in this range, a relatively large amount of CO_2 was absorbed and EC was decreased linearly and steeply to a minimum value of 373 μS/cm at 1 min and 10 s. At the same

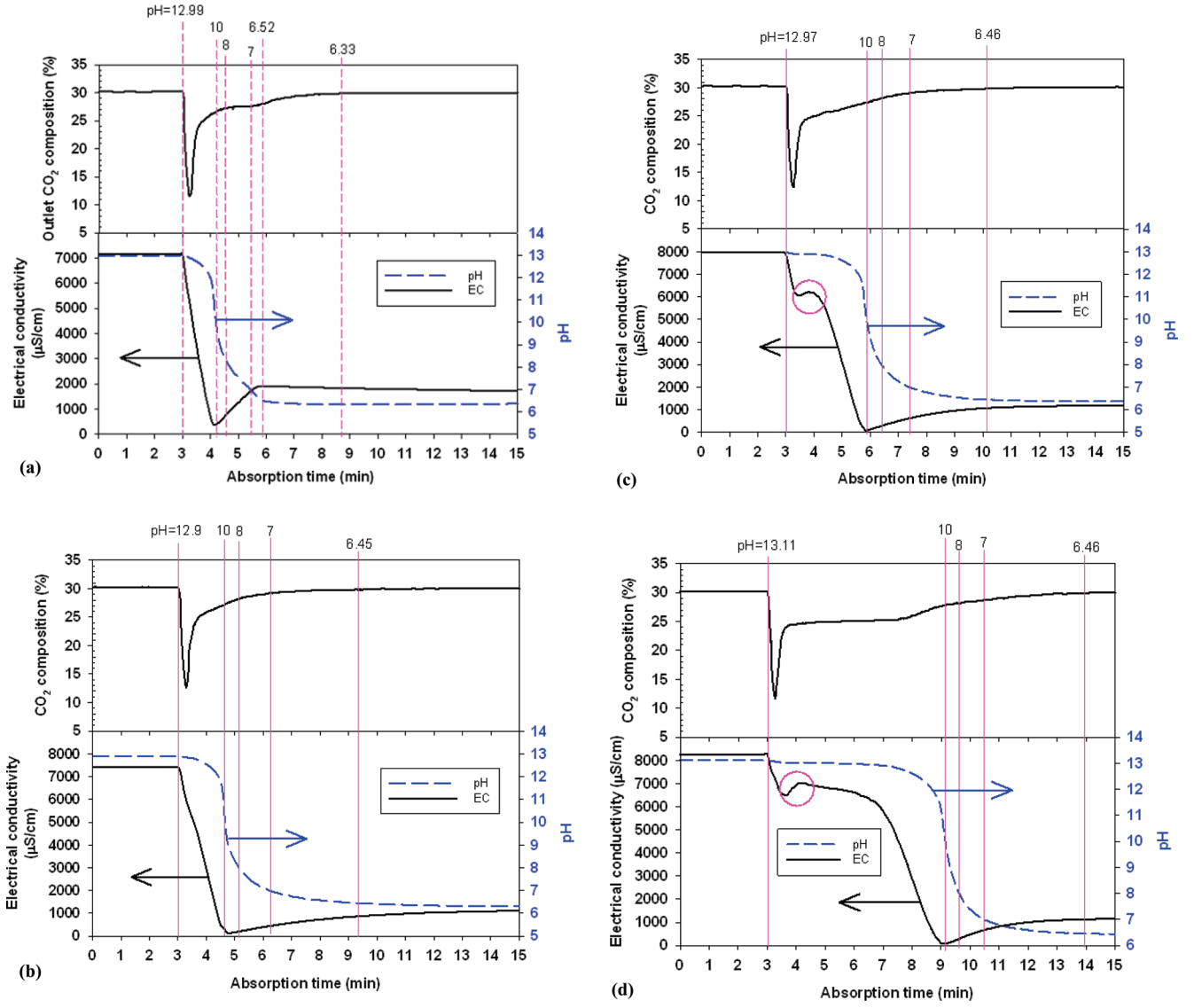

Figure 3. Variation of outlet CO_2 composition, EC, and pH in absorbents according to CO_2 absorption time: (a) 1 g-F, (b) 1 g-S, (c) 2 g-S, and (d) 5 g-S.

time, a pH inflection point of pH 10.46 appeared at the minimum EC point. Therefore, this was the pH range in which $CaCO_3$ was produced by absorbing CO_2, which lowered the concentration in the solution of the ions involved in the $CaCO_3$ production, such as Ca^{2+}, CO_3^{2-}, HCO_3^-, and OH^-.

(2) 8 < pH < 10: In this range, reactions 3−8 proceeded, with reaction 7 dominating, resulting in a higher HCO_3^- concentration. Therefore, $CaCO_3$ was not produced, and the concentration of H^+ and HCO_3^- increased quickly, leading to an EC increase and pH decrease to 8 within a very short time of 30 s.

(3) 7 < pH < 8: In this range, less CO_2 was absorbed and the pH and EC trends were very similar to those of the previous range. However, the pH decrease rate was relatively small because a large amount of OH^- may have already been consumed in the previous range.

(4) pH < 7: CO_2 was continuously absorbed until a pH of 6.33 attained after 3 min and 15 s, which was considered the absorption completion point. However, the EC variation trend in this range was considerably different from that of CO_2 absorption into the $Ca(OH)_2$ suspension solution. Although the EC in all $Ca(OH)_2$ suspension solutions was slowly increased until reaction completion, EC in 1 g-F was increased very quickly until 25 s, after which it was very steadily decreased to the completion point. This phenomenon in this range, therefore, can be explained by dividing into two ranges as follows.

(a) EC increase range; 6.52 < pH < 7: EC at pH 7 was 1684 μS/cm and was increased to 1920 μS/cm at pH 6.52 at 25 s. This was ascribed that a very slight amount of $CaCO_3$ was dissolved to its maximum solubility because of the solution acidity via reaction 11.

(b) EC decrease range; 6.33 < pH < 6.52: Thereafter, EC and pH were simultaneously decreased to 1836 μS/cm and 6.33, respectively. Because the $CaCO_3$ concentration produced in 1 g-F was constant with a relatively small amount, a $CaCO_3$-saturated solution state may be achieved in 6.52 < pH < 7. Therefore, no more $CaCO_3$ can be dissolved in this range, and the compositions of all ions in solution may be controlled to reach the equilibrium state. Therefore, the pH decrease rate was

very small compared to that at 6.52 < pH < 7. In addition, the pH was contrarily and very slightly increased from the pH of 6.33, implying that the range of 6.33 < pH < 6.52 is almost maintained in the equilibrium state.

4.3. CO_2 Absorption in $Ca(OH)_2$ Suspension Solutions. *4.3.1. Using 1g-S as the Absorbent.* The 1 g-S suspension solution comprised 0.7383 g of dissolved $Ca(OH)_2$ coexisting with 0.2618 g of undissolved $Ca(OH)_2$. The initial pH and EC were 12.9 and 7430 μS/cm, respectively. Because EC and pH were measured solely from ions dissolved in the liquid state, the initial EC and pH in 1 g-S should theoretically be the same as those in 1 g-F. However, they were slightly different, which was ascribed to the slight influence exerted by undissolved $Ca(OH)_2$ in suspension on the initial pH and EC. Figure 3b shows the CO_2 absorption, pH, and EC variation with respect to time.

(1) 10 < pH < initial: The absorption behavior in this range was very similar to that of 1 g-F. As absorption began, EC was linearly decreased from the initial value to the minimum of 110.9 μS/cm after 1 min and 45 s. At this time, the pH inflection point appeared at around pH 10, as shown in Figure 3b. The minimum EC point at this point was even smaller than that of 1 g-F (373 μS/cm), because more $CaCO_3$ was produced than in 1 g-F because of the relatively high Ca^{2+} concentration and greater ion consumption for $CaCO_3$ production. Therefore, the minimum EC value decreased with an increasing $Ca(OH)_2$ concentration in suspension, as confirmed in our experiments. Unlike 1 g-F, because reaction 2 proceeded in 1 g-S, the time in this range was 20 s longer than that in 1 g-F and more CO_2 was absorbed.

(2) 7 < pH < 10: The absorption trend of 1 g-S in 8 < pH < 10 was very similar to that in 7 < pH < 8. Reactions in 7 < pH < 10 are theoretically the same as 1 g-F. However, the reaction time in this range was longer and the EC value at pH 7 was lower than that in 1 g-F because more ions participated in the $CaCO_3$ production in the previous range, resulting in fewer remaining ions than in 1 g-F.

(3) pH < 7: Unlike 1 g-F, EC was continuously increased and pH was decreased in this range, indicating that produced $CaCO_3$ was continuously dissolved. Because the concentration of $CaCO_3$ produced in suspension was higher than that in 1 g-F, a continuous supply of CO_2 to the suspension led to continuous dissolution of $CaCO_3$ according to its constant solubility product, resulting in a quasi-equilibrium, in which the EC was steadily increased and the pH was very slowly decreased. The equilibrium state subsequently appeared with constant final values of pH and EC. This phenomenon was commonly observed in all $Ca(OH)_2$ suspensions, and the final EC and pH were approximately 1100 μS/cm and 6.45, respectively.

4.3.2. Using 2g-S−5g-S as the Absorbent. Figure 3c shows the results of the CO_2 absorption in 2 g-S.

Although the CO_2 absorption behavior and pH variation in 2 g-S were very similar to those of 1 g-S, the EC variation was unique in that the EC value rebounded during the $CaCO_3$ production reaction as it decreased from an initial value of 7890 to 6060 μS/cm after 30 s, then increased to 6210 μS/cm after a further 20 s to a small peak, as shown in the small circle of Figure 3c, and finally, decreased again, as in 1 g-S, to an end point at the same rate of 20 s before. The phenomenon of the EC rebound was progressed maintaining the pH at 12.9, which may have been due to undissolved $Ca(OH)_2$. Because 6-fold more $Ca(OH)_2$ remained undissolved in 2 g-S than in 1 g-S, the dissolution rate of $Ca(OH)_2$ may have been faster than that of 1 g-S. In addition, with an excess of undissolved $Ca(OH)_2$ in suspension, the $Ca(OH)_2$ dissolution rate can exceed the $CaCO_3$ precipitation rate. Therefore, an EC rebound should be observed in all suspensions with a $Ca(OH)_2$ concentration higher than that in 2 g-S, and this was confirmed in our experiments. For example, Figure 3d shows the EC rebound in 5 g-S.

An EC rebound was also observed around pH 12.9, after which the EC slightly and steadily decreased until 3 min in the same manner as in 2 g-S. The longer time of 3 min was due to its higher $Ca(OH)_2$ concentration compared to that of 2 g-S. Therefore, in CO_2 absorption using $Ca(OH)_2$ suspension, the $Ca(OH)_2$ dissolution rate significantly affected the $CaCO_3$ production rate, resulting in an EC increase or decrease during the reaction.

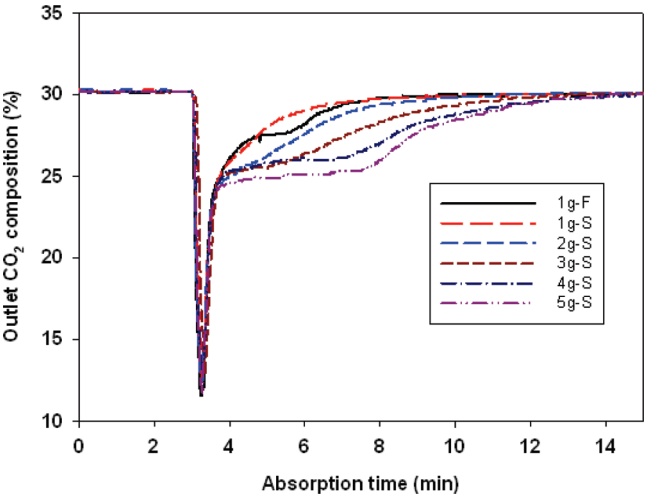

Figure 4. Absorption behavior of CO_2 in each absorbent according to absorption time.

Table 1. Total and Individual Amount of CO_2 Absorbed in Each Absorbent According to the pH Range

	CO_2 absorbed in absorbents (g of CO_2)					
pH ranges	1 g-F	1 g-S	2 g-S	3 g-S	4 g-S	5 g-S
10 < pH < initial	0.666	0.763	1.179	1.535	2.049	2.421
8 < pH < 10	0.122	0.079	0.097	0.104	0.074	0.088
7 < pH < 8	0.103	0.123	0.127	0.140	0.122	0.123
final < pH < 7	0.234	0.126	0.148	0.192	0.241	0.244
total	1.125	1.091	1.551	1.971	2.486	2.876
(7 < pH < 10)	0.225	0.202	0.224	0.244	0.196	0.211
(final < pH < 10)	0.459	0.328	0.372	0.436	0.437	0.455

4.4. Amount of Absorbed CO_2. Figure 4 shows the absorption behavior of CO_2 in each absorbent.

The amount of absorbed CO_2, calculated by integrating the area enclosed by the line of outlet CO_2 composition, increased linearly with an increasing $Ca(OH)_2$ concentration in the absorbent. In addition, its individual values in the pH ranges are summarized in Table 1.

The amount of CO_2 absorbed in 10 < pH < initial was increased with respect to the $Ca(OH)_2$ concentration in the absorbent, as shown in the first row of the table, because $CaCO_3$ was produced in this range. However, the amount of CO_2 absorbed in final < pH < 10 was similar in all absorbents at approximately 0.4 g of CO_2, as shown in the last row of the table. This is an important result for CO_2 absorption in a $Ca(OH)_2$

dx.doi.org/10.1021/ef200415p |*Energy Fuels* 2011, 25, 3825–3834

Table 2. Theoretical and Experimental Value of CO_2 Consumed in Terms of $CaCO_3$ Production

absorbent	theoretical amount of CO_2 consumed solely to produce $CaCO_3$ (g)	consumed CO_2 not involved in $CaCO_3$ production (calculated) (g)	experimental amount of CO_2 consumed solely to produce $CaCO_3$ (g)	additional amount of CO_2 required to convert all $Ca(OH)_2$ to $CaCO_3$ production (g)	g of CO_2 absorbed in 10 < pH < initial/g of $Ca(OH)_2$ fed in solution
1 g-F	0.439	0.686	0.439	0.000	0.902
1 g-S	0.595	0.496	0.404	0.191	0.763
2 g-S	1.189	0.362	0.865	0.324	0.590
3 g-S	1.784	0.187	1.285	0.499	0.512
4 g-S	2.378	0.108	1.799	0.579	0.512
5 g-S	2.973	−0.097	2.189	0.784	0.484

aqueous solution system. In 1 g-F, theoretical CO_2 required to convert $Ca(OH)_2$ to $CaCO_3$ was calculated as 0.439 g via reaction 1. However, the amount of CO_2 absorbed in 10 < pH < initial, where $CaCO_3$ was produced, was measured as 0.666 g in our experiment. Therefore, 0.227 g was absorbed irrespective of the $CaCO_3$ production. In addition, 0.459 g of CO_2 absorbed in final < pH < 10, as listed in Table 1, was not related to the $CaCO_3$ production, either. Therefore, 0.686 g of absorbed CO_2 did not participate in the $CaCO_3$ production in 1 g-F; i.e., this was physically solved and consumed to produce various ions not involved in $CaCO_3$ production.

Applying the same logic to all suspension absorbents, CO_2 consumed solely to produce $CaCO_3$ in each suspension can be calculated as listed in the second column of Table 2.

Therefore, when this value was subtracted from the total amount of absorbed CO_2 calculated from the experiment in each suspension, the amount of absorbed CO_2 not involved in the $CaCO_3$ production, as listed in the third column of Table 2, was 0.496 g in 1 g-S and, in the other four suspension absorbents, it decreased with an increasing $Ca(OH)_2$ concentration to a negative value for 5 g-S. However, this result could not be explained because the amount of CO_2 absorbed irrespective of $CaCO_3$ production in all absorbents should theoretically only be slightly different. This was verified from the experiment in which the final pH and EC, after completion of $CaCO_3$ production, converged to a constant value with the quasi-steady state in every suspension absorbent.

Therefore, 0.686 g of CO_2, which was calculated from 1 g-F, was assumed to be CO_2 commonly absorbed in all absorbents not directly involved in $CaCO_3$ production. When this value was subtracted from the total amount of CO_2 absorbed in each solution measured from the experiment, the net amount of CO_2 solely consumed for $CaCO_3$ production in each solution was calculated, as listed in the fourth column of Table 2. All suspensions exhibited smaller values than the theoretical value, and the difference between them increased with an increasing $Ca(OH)_2$ concentration, as listed in the fifth column of Table 2. This indicated that Ca^{2+} in suspension may not have been sufficiently associated with CO_3^{2-} or that a very small amount of $Ca(OH)_2$ may have remained unconverted to $CaCO_3$. Possibly, undissolved $Ca(OH)_2$ may have been instantaneously covered with precipitating $CaCO_3$ in the production step, and some $CaCO_3$ may have been synthesized on the surface of undissolved $Ca(OH)_2$, as presented in the shrinking core model.

The total amount of CO_2 absorbed in 1 g-F was larger than that of 1 g-S, which was explained as follows. Ca^{2+} and CO_3^{2-} in 1 g-F reacted with each other as the ion state in solution, thereby producing rhombohedral $CaCO_3$ with very high crystallinity and

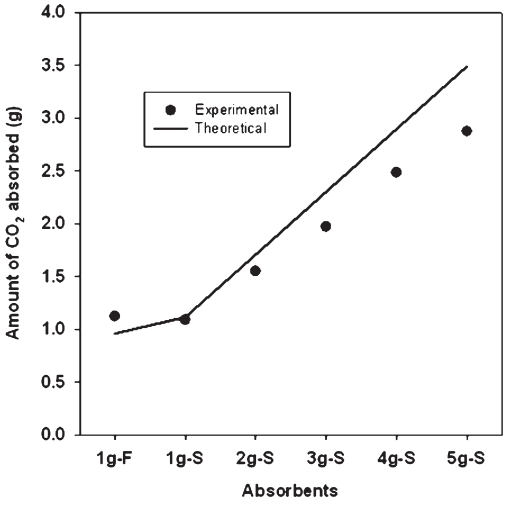

Figure 5. Theoretical and experimental amount of CO_2 absorbed in each absorbent.

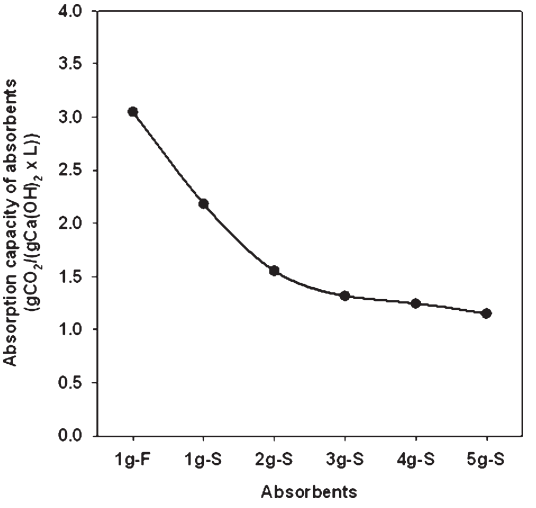

Figure 6. CO_2 absorption capacity of absorbents calculated on the basis of the amount of $Ca(OH)_2$ fed in solution and the volume of absorbents.

density. On the other hand, in 1 g-S, the simultaneous $Ca(OH)_2$ dissolution and $CaCO_3$ production may have substantially hindered the association between Ca^{2+} and CO_3^{2-} in suspension and the reaction may not have been fully completed. Therefore, absorbed CO_2 that solely participated in the $CaCO_3$ production, 0.404 g, was slightly lower than that of 1 g-F, resulting in the

production of less crystallized $CaCO_3$. Consequently, the amount of absorbed CO_2 that directly participated in the $CaCO_3$ production was less than the theoretical value at high concentrations of $Ca(OH)_2$ in suspension.

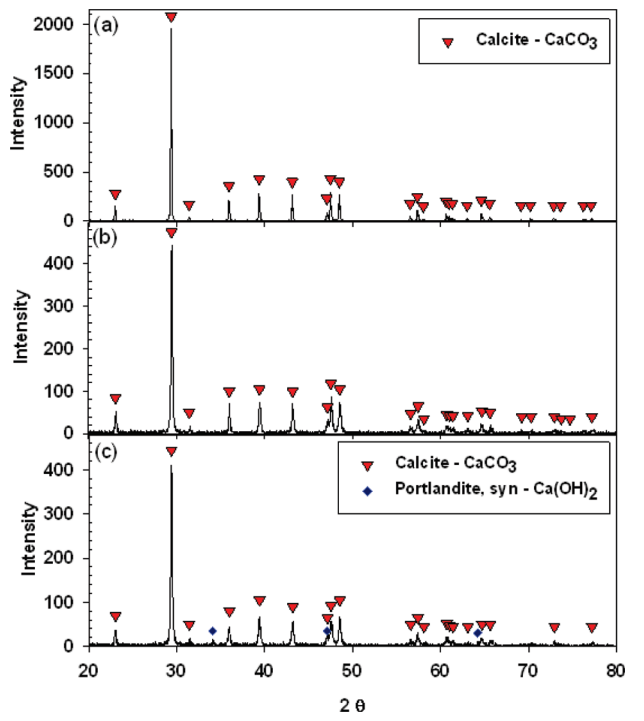

Figure 7. XRD patterns of $CaCO_3$ produced in the absorbents: (a) 1 g-F, (b) 1 g-S, and (c) 5 g-S.

The following experimental data supported this explanation: the value of the amount of CO_2 absorbed in 10 < pH < initial divided by the amount of $Ca(OH)_2$ fed in the solution. This value was directly proportional to CO_2 consumed in the $CaCO_3$ production, and the values for the six absorbents are listed in the final column of Table 2. They were decreased with an increasing $Ca(OH)_2$ concentration to a minimum of 0.484 g of CO_2/g of $Ca(OH)_2$ for 5 g-S, indicating that highly concentrated $Ca(OH)_2$ in suspension deteriorated the CO_2 absorption for $CaCO_3$ production.

Figure 5 compares the theoretical and experimental amounts of CO_2 absorbed in the absorbents.

The theoretical value is the sum of CO_2 required to produce $CaCO_3$ via reaction 1 and CO_2 absorbed into pure water. The experimental values in 1 g-F and 1 g-S were 117 and 98% of the theoretical value, respectively. In 5 g-S, it was further decreased to 82%. Meanwhile, CO_2 absorbed in 1 g-F may have been fully consumed to produce $CaCO_3$ and, hence, was fully saturated in water to its theoretical value. In addition, the excess of absorbed CO_2 over the theoretical value may have generated various additional ions, such as HCO_3^- and CO_3^{2-}, which cannot be further associated with Ca^{2+} because of its depletion. Therefore, the amount of CO_2 absorbed in 1 g-F was 17% larger than the theoretical value, which corresponds to 0.166 g of CO_2 among the total absorbed CO_2. In suspension, however, because not as much $CaCO_3$ was produced as its theoretical value because of $Ca(OH)_2$ hindrance, the amount of absorbed CO_2 was less than

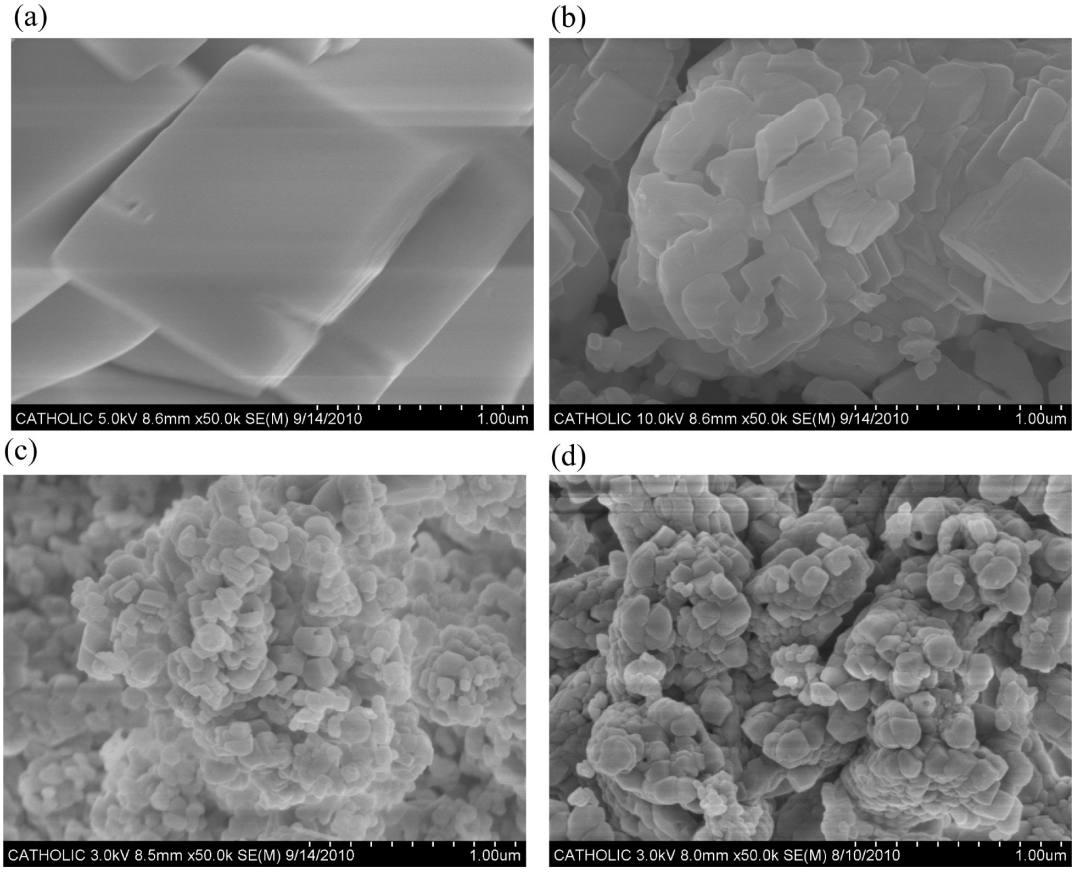

Figure 8. SEM photographs of $CaCO_3$ produced in the absorbents: (a) 1 g-F, (b) 1 g-S, (c) 2 g-S, and (d) 5 g-S.

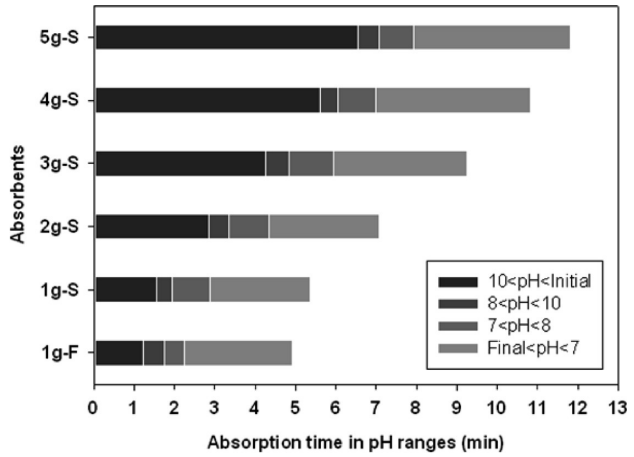

Figure 9. Absorption time of each absorbent in the pH ranges.

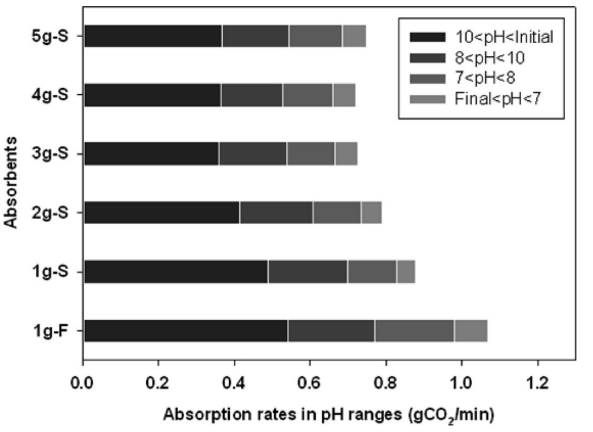

Figure 10. Absorption rates of each absorbent in the pH ranges.

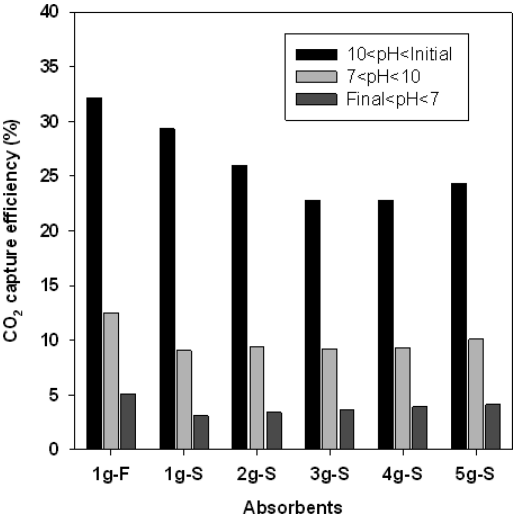

Figure 11. CO_2-capture efficiencies of each absorbent in the pH ranges.

the theoretical value. Therefore, the higher $Ca(OH)_2$ concentration in suspension reduced the CO_2 absorption capacity of the absorbents. Figure 6 shows the absorption capacity of the absorbents based on the amount of $Ca(OH)_2$ fed in the solution and the volume of absorbents.

The calculated value of 1 g-F of 3.05 g of CO_2 [g of $Ca(OH)_2]^{-1}$ L^{-1} was 1.5- and 3-fold more than that of 1 g-S and 5 g-S, respectively. This confirmed $Ca(OH)_2$-saturated aqueous solution as the best absorbent in terms of CO_2 absorption capacity.

4.5. XRD and SEM Analysis of Produced $CaCO_3$. Figure 7 shows the XRD patterns of $CaCO_3$ produced in each absorbent.

The intensity of the XRD patterns revealed that, whereas $CaCO_3$ synthesized in 1 g-F was very highly crystallized, that synthesized in 1 g-S and 5 g-S was less crystallized. The XRD patterns of $CaCO_3$ produced in 2 g-S, 3 g-S, and 4 g-S were the same as those of 1 g-S. In addition, no peaks from $Ca(OH)_2$ were found in $CaCO_3$ produced in suspension. However, two or three very tiny peaks, possibly attributable to $Ca(OH)_2$, are shown as the tracer level in Figure 7c.

Figure 8 shows SEM images of the morphology of $CaCO_3$ produced in the solution.

$CaCO_3$ produced in 1 g-F was clearly depicted as rhombohedral calcite with very high crystallinity.[52] On the other hand, $CaCO_3$ manufactured in 2 g-S−5 g-S was more agglomerated with a small and non-uniform particle size. The morphology of $CaCO_3$ produced in 3 g-S and 4 g-S was almost the same as that of 2 g-S and 5 g-S. Meanwhile, $CaCO_3$ produced in 1 g-S exhibited an intermediate shape between 1 g-F and 2 g-S in terms of particle size and agglomeration. These results demonstrated that the $Ca(OH)_2$ concentration in solution affected the CO_2 absorption and, hence, the morphology of precipitated $CaCO_3$.

4.6. Absorption Time and Rate. Figure 9 shows the total and individual absorption times of each absorbent in the pH ranges.

The absorption time in 10 < pH < initial was positively correlated with the $Ca(OH)_2$ concentration in solution. Although the absorption time of 1 g-F in 7 < pH < 10 was 1 min, the absorption time of all suspensions in this range was constant at 1 min and 30 s. In other words, the absorption time in this range was not directly related to the $Ca(OH)_2$ concentration in suspension because CO_2 was saturated in this range because of the completion of the $CaCO_3$ production in the previous range. However, the absorption time in final < pH < 7 was increased slightly with an increasing $Ca(OH)_2$ concentration in suspension because $CaCO_3$ was produced in proportion to the $Ca(OH)_2$ concentration in suspension, and CO_2 absorbed in this range was consumed to dissolve $CaCO_3$ in the quasi-equilibrium state.

Figure 10 shows the absorption rate of all absorbents in the pH ranges.

The 1 g-F absorbent exhibited the largest absorption rate in 10 < pH < initial of 0.54 g of CO_2/min. The rate in suspensions linearly decreased with an increasing $Ca(OH)_2$ concentration to 0.36 g of CO_2/min for 3 g-S and was then maintained at a constant value for 4 g-S and 5 g-S. This implied that $Ca(OH)_2$ dissolution substantially delayed the $CaCO_3$ production rate, suggesting that it may be the rate-controlling step of CO_2 absorption in suspension. However, the $CaCO_3$ production rate was not influenced by $Ca(OH)_2$ in suspension at concentrations over 0.4 wt % (2 g-S). In addition, the local rates in 7 < pH < 10 and final < pH < 7 of all suspension absorbents were the same at 0.15 and 0.05 g of CO_2/min, respectively. However, the rate of 1 g-F in pH < 10 was higher than that of the other five suspensions because the absolute amount of CO_2 absorbed in 10 < pH < initial was relatively small compared to that of the suspension system, and the value of the consumed $CO_2/Ca(OH)_2$ was the

largest, which reduced the CO_2 concentration per volume of solution. Therefore, to compensate for this CO_2 concentration shortage for saturation in 1 g-F, CO_2 may have been more quickly absorbed in final < pH < 7 than in a suspension system.

4.7. CO_2-Capture Efficiency. Figure 11 shows the CO_2-capture efficiency of the absorbent, which is the ratio of the amount of CO_2 absorbed in solution to that in the feeding gas mixture, in the pH ranges.

The calculated maximum value was 32.17% for 1 g-F in 10 < pH < initial, and it linearly decreased with an increasing $Ca(OH)_2$ concentration to 3 g-S and was then maintained almost constant for 4 g-S and 5 g-S. In addition, the capture efficiency of 1 g-F in the other pH ranges was also larger than that of the other five suspensions. These results demonstrated that 1 g-F was the most efficient absorbent to capture CO_2 in a $Ca(OH)_2$ aqueous solution system.

5. CONCLUSION

The present paper has investigated the CO_2-capture performance of $Ca(OH)_2$ aqueous solution as an absorbent via the absorption of a gas mixture with a CO_2 composition of about 30%. In the study results, the $Ca(OH)_2$ concentration in the solution strongly affected the CO_2-capture performance of the absorbent.

The excess of undissolved $Ca(OH)_2$, which existed in suspension, significantly degraded the CO_2 absorption, which was primary ascribed to the effect of the simultaneous $Ca(OH)_2$ dissolution and $CaCO_3$ production in hindering the association between Ca^{2+} and CO_3^{2-} in suspension. Therefore, the CO_2 absorption resulting in $CaCO_3$ precipitation was restricted by the $Ca(OH)_2$ dissolution rate, and a higher $Ca(OH)_2$ concentration in suspension further reduced the CO_2 absorption capacity of the absorbents and produced substantially agglomerated $CaCO_3$ with low crystallinity.

In contrast, the $Ca(OH)_2$-saturated aqueous solution, 1 g-F, absorbed more CO_2 than the theoretical amount. The absorption rate and capture ratio of 1 g-F in 10 < pH < initial, at 0.54 g of CO_2/min and 32.17%, respectively, were the highest among all six absorbents. In addition, the calculated absorption capacity of 1 g-F, at 3.05 g of CO_2 [g of $Ca(OH)_2]^{-1}$ L^{-1}, was 3-fold more than that of the 5 g-S absorbent, which confirmed $Ca(OH)_2$-saturated aqueous solution as the most efficient absorbent for CO_2 capture in a $Ca(OH)_2$ aqueous solution system.

AUTHOR INFORMATION

Corresponding Author

*Telephone: +82-2-2164-4866. Fax: +82-2-2164-4765. E-mail: jhwee@catholic.ac.kr or jhwee@korea.ac.kr.

ACKNOWLEDGMENT

This research was supported by the Basic Research Program through the National Research Foundation of Korea (NRF) funded by the Ministry of Education, Science, and Technology (2010-0009938), as well as supported by the Catholic University of Korea, Research Fund, 2011.

REFERENCES

(1) Metz, B.; Ogunlade, D.; Heleen, C. D. C. In *Intergovernmental Panel on Climate Change (IPCC) Special Report on Carbon Dioxide Capture and Storage*; Loos, M., Meyer, L. A., Eds.; Cambridge University Press: Cambridge, U.K., 2005; p 442.

(2) Klemeš, J.; Bulatov, I.; Cockerill, T. *Comput. Chem. Eng.* **2007**, *31*, 445–455.

(3) Sada, E.; Kumazawa, H.; Osawa, Y.; Matsuura, M.; Han, Z. Q. *Chem. Eng. J.* **1986**, *33*, 87–95.

(4) Saha, A. K.; Bandyopadhyay, S. S.; Biswas, A. K. *Chem. Eng. Sci.* **1997**, *50*, 3587–3598.

(5) Barchas, R.; Davis, R. *Energy Convers. Manage.* **1992**, *33*, 333–340.

(6) Sander, M. T.; Mariz, C. L. *Energy Convers. Manage.* **1992**, *33*, 341–348.

(7) Kosugi, T.; Hayashi, A.; Matsumoto, T.; Akimoto, K.; Tokimatsu, K.; Yoshida, H.; Tomoda, T.; Kaya, Y. *Energy* **2004**, *29*, 1297–1308.

(8) Alie, C.; Backham, L.; Croiset, E.; Douglas, P. L. *Energy Convers. Manage.* **2005**, *46*, 475–487.

(9) Kim, Y. S.; Yang, S. M. *Sep. Purif. Technol.* **2000**, *21*, 101–109.

(10) Anand, B. R.; Edward, S. R. *Environ. Sci. Technol.* **2002**, *36*, 4467–4475.

(11) Bishnoi, S.; Rochelle, G. T. *Chem. Eng. Sci.* **2000**, *55*, 5531–5543.

(12) Satyapal, S.; Filburn, T.; Trela, J.; Strange, J. *Energy Fuels* **2001**, *15*, 250–255.

(13) Sharp, W. E.; Kennedy, G. C. *J. Geol.* **1965**, *73*, 391–403.

(14) Juvekar, V. A.; Sharma, M. M. *Chem. Eng. Sci.* **1973**, *28*, 825–837.

(15) Chen, J. C.; Fang, G. C.; Tang, J. T.; Liu, L. P. *Chemosphere* **2005**, *59*, 99–105.

(16) Yagi, H.; Okamoto, K.; Naka, K.; Hikita, H. *Chem. Eng. Commun.* **1984**, *26*, 1–9.

(17) Park, S. Y.; Choi, W. S. *Adv. Powder Technol.* **2004**, *15*, 1–12.

(18) Kakaraniya, S.; Gupta, A.; Mehra, A. *Ind. Eng. Chem. Res.* **2007**, *46*, 3170–3179.

(19) Yang, J. H.; Shih, S. M.; Wu, C. I.; Tai, Y. D. C. *Powder Technol.* **2010**, *202*, 101–110.

(20) Seo, K.-S.; Han, C.; Wee., J.-H.; Park, J.-K.; Ahn, J.-W. *J. Cryst. Growth* **2005**, *276*, 680–687.

(21) Kakizawa, M.; Yamasaki, A.; Yanagisawa, Y. *Energy* **2001**, *26*, 341–354.

(22) Zhang, J.; Zhang, R.; Geerlings, H.; Bi, J. *Chem. Eng. Technol.* **2010**, *33*, 1177–1183.

(23) Ptáček, P.; Nosková, M.; Brandštetr, J.; Šoukal, F.; Opravil, T. *Thermochim. Acta* **2010**, *498*, 54–60.

(24) Rendek, E.; Ducom, G.; Germain, P. *J. Hazard. Mater.* **2006**, *128*, 73–79.

(25) Freyssinet, Ph.; Piantone, P.; Azaroual, M.; Itard, Y.; Clozel-Leloup, B.; Guyonnet, D.; Baubron, J. C. *Waste Manage.* **2002**, *22*, 159–172.

(26) Huijgen, W. J.; Witkamp, G. J.; Comans, R. N. *Environ. Sci. Technol.* **2005**, *39*, 9676–9682.

(27) Teir, S.; Eloneva, S.; Fogelholm, C. J.; Zevenhoven, R. *Energy* **2007**, *32*, 528–539.

(28) Anthony, E. J. *Greenhouse Gas Sci. Technol.* **2011**, *1*, 36–47.

(29) Van Balen, K. *Cem. Concr. Res.* **2005**, *35*, 647–657.

(30) Beruto, D. T.; Botter, R. *J. Eur. Ceram. Soc.* **2000**, *20*, 497–503.

(31) Shih, S. H.; Ho, C. S.; Song, Y. S.; Lin, J. P. *Ind. Eng. Chem. Res.* **1999**, *38*, 1316–1322.

(32) Steinfeld, A.; Thompson, G. *Energy* **1994**, *19*, 1077–1081.

(33) Halmann, M.; Steinfeld, A. *Energy Fuels* **2003**, *17*, 774–778.

(34) Halmann, M.; Steinfeld, A. *Energy* **2006**, *31*, 1533–1541.

(35) Nikulshina, V.; Hirsch, D.; Mazzotti, M.; Steinfeld, A. *Energy* **2006**, *31*, 1715–1725.

(36) Blamey, J.; Anthony, E. J.; Wang, J.; Fennell, P. S. *Prog. Energy Combust.* **2010**, *36*, 260–279.

(37) Słowiński, G. *Int. J. Hydrogen Energy* **2006**, *31*, 1091–1102.

(38) Wang, Y. D.; Huang, Y.; McIlveen-Wright, D.; Hewitt, N.; Eames, P.; Rezvani, S.; McMullan, J. *Fuel* **2006**, *85*, 2133–2140.

(39) Dubey, M. K.; Ziock, H.; Rueff, G.; Elliott, S.; Smith, W. S. *Prepr. Pap.—Am. Chem. Soc., Div. Fuel Chem.* **2002**, *47*, 81–84.
(40) Zeman, F. S.; Lackner, K. S. *World Resour. Rev.* **2004**, *16*, 157–172.
(41) Zeman, F. *Environ. Sci. Technol.* **2007**, *41*, 7558–7563.
(42) Gupta, H.; Fan, L. S. *Ind. Eng. Chem. Res.* **2002**, *41*, 4035–4042.
(43) Bassett, H. *J. Chem. Soc.* **1934**, 1270–1275.
(44) Perry, R. H.; Green, D. W. *Perry's Chemical Engineers' Handbook*, 8th ed.; McGraw-Hill: New York, 2008; pp 2—126.
(45) Park, J. W.; Kim, J. S.; Ahn, J. W.; Han, C. J. *Ind. Eng. Chem. (Seoul, Repub. Korea)* **2006**, *17*, 67–72.
(46) Ahn, J. W.; Park, C. H.; Kim, J. H.; Lee, J. K.; Kim, H. *J. Korean Assoc. Cryst. Growth* **1996**, *6*, 509–520.
(47) Quinn, E. L.; Jones, C. L. *Carbon Dioxide*; Reinhold Publishing Corporation: New York, 1936.
(48) Keene, F. R. In *Electrochemical and Electrocatalytic Reactions of Carbon Dioxide*; Sullivan, B. P., Krist, K., Guard, H. E., Eds.; Elsevier: Amsterdam, The Netherlands, 1993; pp 1—18.
(49) Yoo, D. S.; Kang, S. W.; Lee, K. R. *Geosyst. Eng.* **1997**, *34*, 60–73.
(50) Montes-Hernandez, G.; Fernández-Martínez, A.; Charlet, A.; Tisserand, D.; Renard, D. *J. Cryst. Growth* **2008**, *310*, 2946–2953.
(51) Plummer, L. N.; Busenberg, E. *Geochim. Cosmochim. Acta* **1982**, *46*, 1011–1040.
(52) Lyu, S. G.; Ryu, S. O.; Park, Y. H.; Rhew, J. H.; Sur, G. S. J. *Ind. Eng. Chem.* **1998**, *36*, 543–547.